

COHERENT X-RAY DIFFRACTIVE IMAGING AT THE ADVANCED LIGHT SOURCE



H. Chapman, S. Marchesini, S. Hau-Riege, A. Barty



M. Howells, H. He, H.A. Padmore, C. Cui, J. Holton, R.M. Glaeser



J.C.H. Spence, U. Weierstall



C. Jacobsen, J. Kirz, D. Sayre, D. Shapiro, T. Beetz, E. Lima



V. Elser, P. Thibault

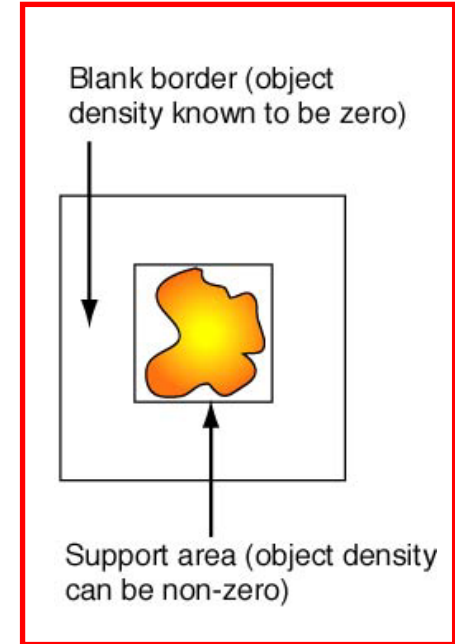
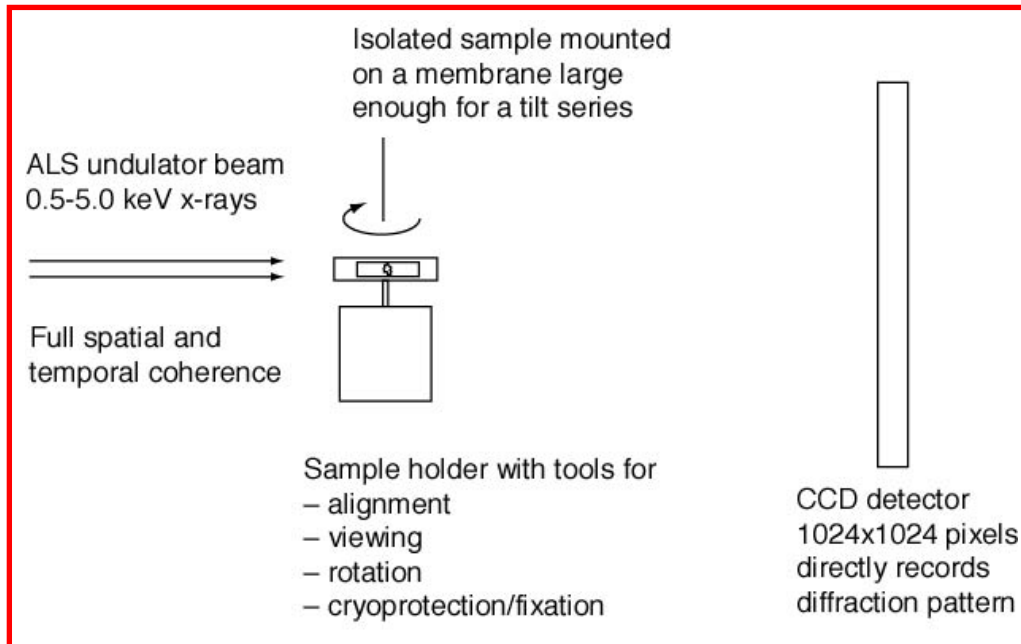
What is CXDI?

- Coherent X-ray diffractive imaging (CXDI) is a lensless imaging technique.
- Diffraction patterns of isolated objects are recorded and their images reconstructed by iterative algorithms.

Why is it useful?

- 3D imaging of 0.5-20 μm isolated objects
- Objects that are too thick for Electron Microscopy e.g. 10 μm (1024 cube at 10nm resolution means 10 microns thickness)
- Objects that are too thick for zone-plate tomographic X-ray microscopy (depth of focus $< 1 \mu\text{m}$ at 10 nm resolution for soft X-rays even if zone plates become available)

WHAT IS COHERENT X-RAY DIFFRACTION IMAGING?

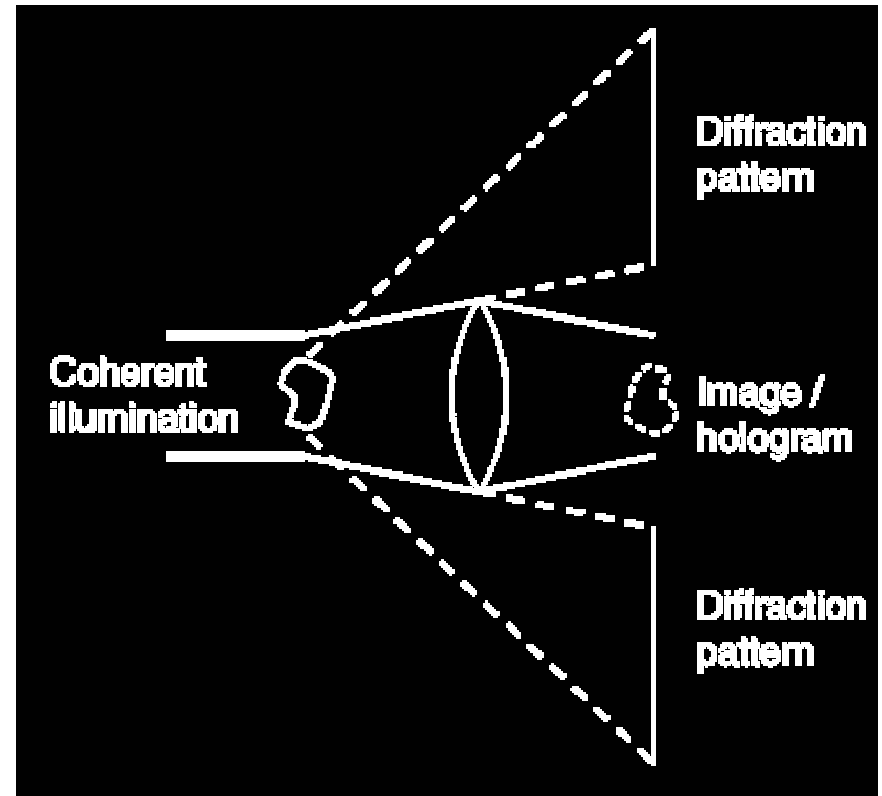


- A 2D CXDI experiment consists of recording a far-field diffraction pattern with coherent x-rays
- The reconstruction is made using a 2D phase-retrieval algorithm that transforms back and forth between the object plane and the diffraction plane
 - object plane - enforce that the object lies inside a known “support area”
 - diffraction plane - enforce that the diffraction intensities agree with the measured pattern
- A 3D experiment consists of a tilt series of about 180 such patterns plus a 3D algorithm
- Several successful 3D experiments now done (by us and others) mostly on test objects

IMAGING BEYOND THE LENS LIMITS?



- **Recording images:**
 - No phase problem, the lens Fourier transforms the complex scattered wavefield.
 - Lens introduces aberrations.
 - The numerical aperture of the lens limits resolution.
- **Recording diffraction patterns:**
 - Phase problem, only modulus of complex scattered wavefield is recorded.
 - No lens-imposed resolution limits!
 - No aberrations!



GOALS



<10 nm resolution (3D) in 1 - 10 μ m size biological specimens
(frozen hydrated cells, organelles)

Resolution limits imposed by radiation damage!

< 3 nm resolution in less sensitive nanostructures
(Inclusions, porosity, clusters, composite nanostructures, aerosols...)
eg: molecular sieves, catalysts, crack propagation, mesoporous structures

HISTORY



Sayre (1952) - observation that Bragg diffraction undersamples diffracted intensity relative to Shannon's theorem

Gerchberg and Saxton (1972) - First iterative phase-retrieval algorithm successful on test data

Sayre (1980) - Idea to do "crystallography" with non-periodic objects (i. e. attempt phase retrieval) and exploit the cross-section advantage of soft x-rays

Sayre, Yun, Chapman, Miao, Kirz (1980's and 1990's) - development of the experimental technique

Bates (1982-4) - Idea to oversample the wave amplitude to produce a zero-padded border around the object

Fienup (1980's) - Development of practical phase-retrieval algorithms including use of the support constraint

Miao, Charalambous, Kirz and Sayre (1999) - demonstration of 2-D microscopy using a Fienup-style algorithm at 0.73 keV x-ray energy, 0.07 μm resolution

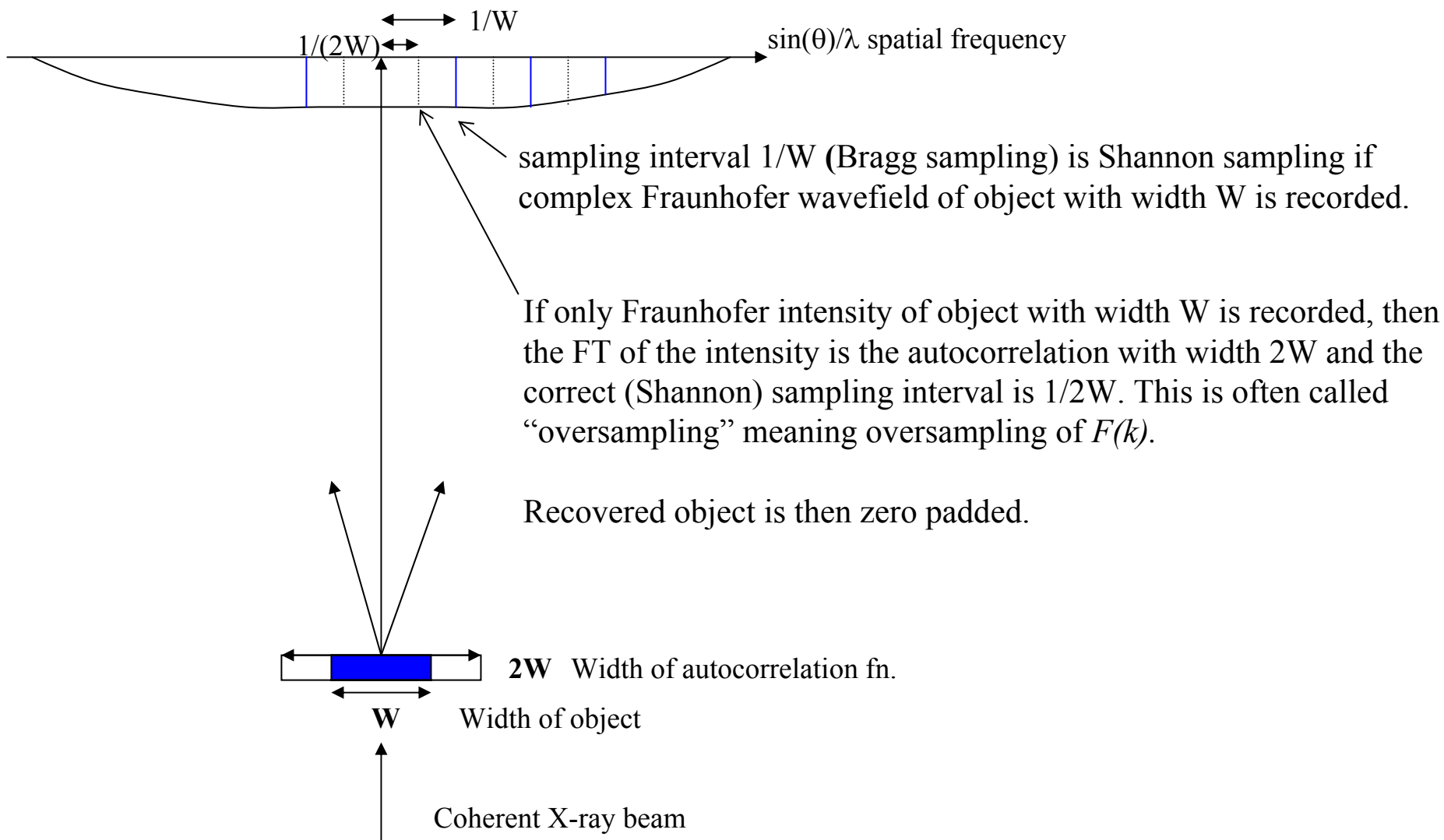
Miao et al (2001) - use of harder x-rays - 5.5 keV
improved resolution in 2-D: 7 nm
achievement of 3-D with resolution 55 nm

He et al (2002) - reconstruction without use of other microscopes for determination of either (a) the support or (b) the lower frequency data

THE BASIC IDEA - “OVERSAMPLING” SOLVES THE PHASE PROBLEM.



Shannon sampling theorem: if a function $f(x)$ with transform $F(k)$ is bounded on one side with width W , then the function on the other side can be fully recovered from samples spaced at $1/W$



PHASE-RETRIEVAL ALGORITHMS: GENERAL SCHEME



REAL SPACE
 $f(\mathbf{x})$

FOURIER SPACE
 $F(\mathbf{k})$

Apply object-space constraints
(known support) - get first
estimate of $f(\mathbf{x})$: $g_1(\mathbf{x})$

Measured data
Add random
phases

Starting point

FFT⁻¹

i-th iteration

IN $g_i(\mathbf{x})$

FFT

$G_i(\mathbf{k})$

1

2

Fourier domain constraints
(measured magnitudes)

$g'_i(\mathbf{x})$

FFT⁻¹

$G'_i(\mathbf{k})$

3

Object domain constraints
(known support)

4

OUT $g_{i+1}(\mathbf{x})$

First atomic-resolution image of a DWNT by Electron Microscopy obtained using diffractive imaging with HIO reconstruction.

Aberration-free.

Gives ID, OD, Chiral vectors.

Zuo et al
Science, 2003.

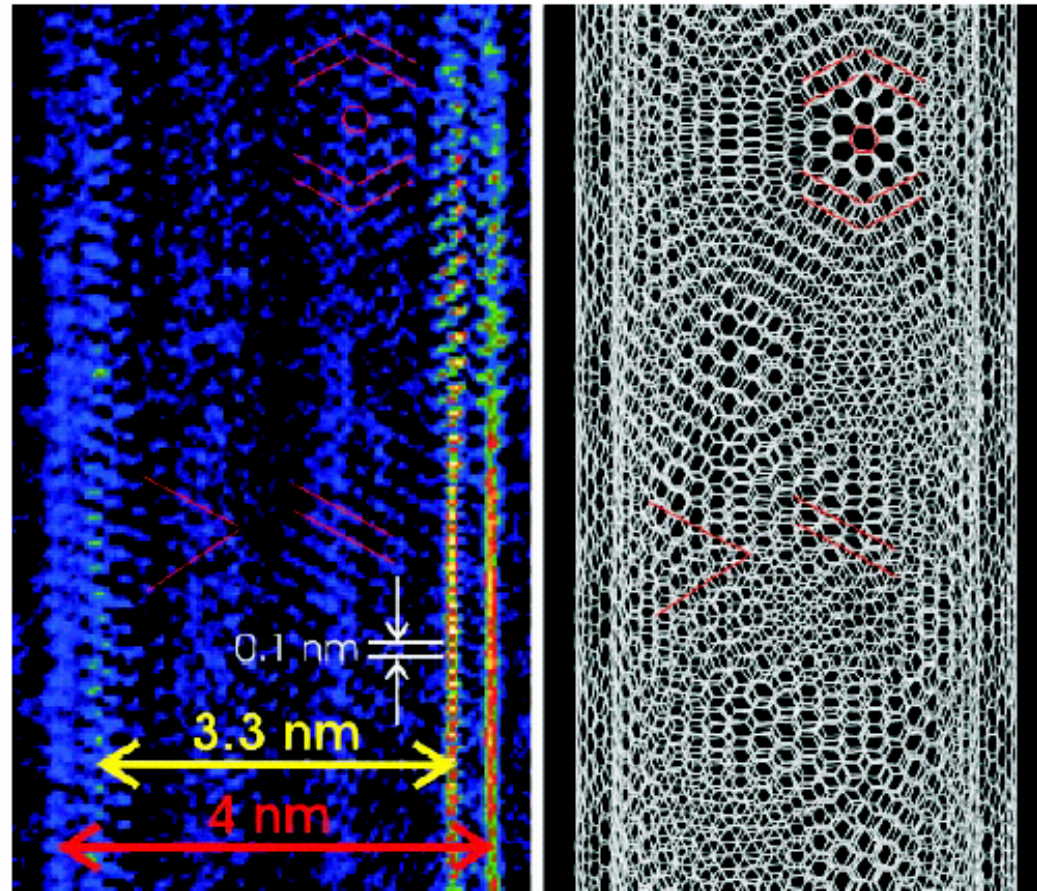
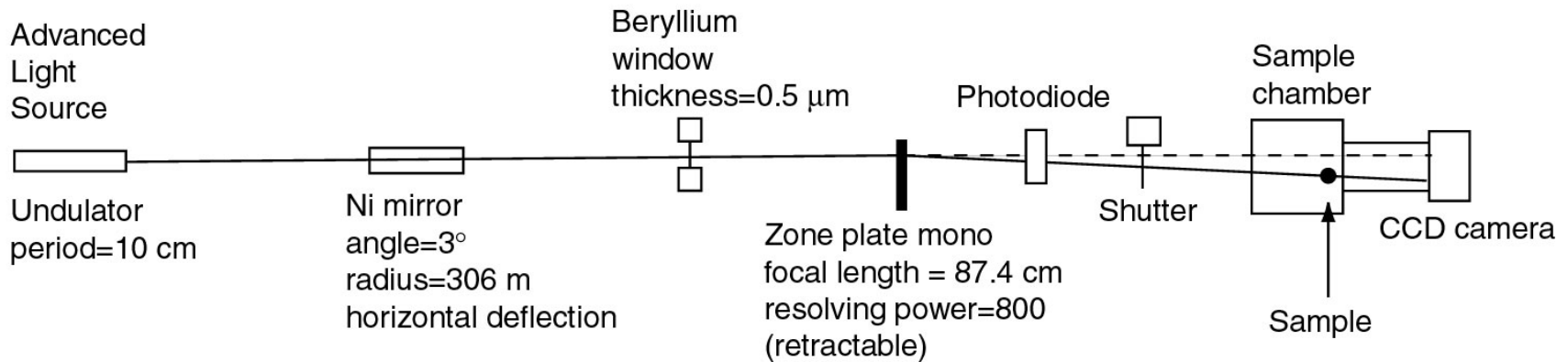


Fig. 2. (left) A section of the reconstructed DWNT image at 1-Å resolution and (right) a structural model constructed with the use of the chiral vectors of (35, 25) and (26, 24) that were determined from the image and diffraction pattern. The DWNT imaged here is one of many in our catalytic chemical vapor deposition-grown samples. Yellow and red lines mark the diameters of the inner and outer tubes, respectively. One side of walls is stronger than the other, which is because of the illumination. The DWNT is incommensurate. In projection, the structure has complex patterns showing both accidental coincidences and Moiré fringes, which are highlighted by hexagons and lines.

ALS BEAM LINE 9.0.1 COHERENT OPTICS



BEAM LINE SIDE VIEW (NOT TO SCALE)

NOTES:

- Our latest experiments are done at 750 eV in undulator 3rd harmonic
- Be window and zone-plate monochromator both 0.8 mm in size are designed to withstand pink (once reflected) beam
- Diffractive elements of the zone plate monochromator (Charalambous, Yun) made of silicon nitride coated on both sides with Copper for better mechanical stability and heat removal

Details beamline 9.0.1

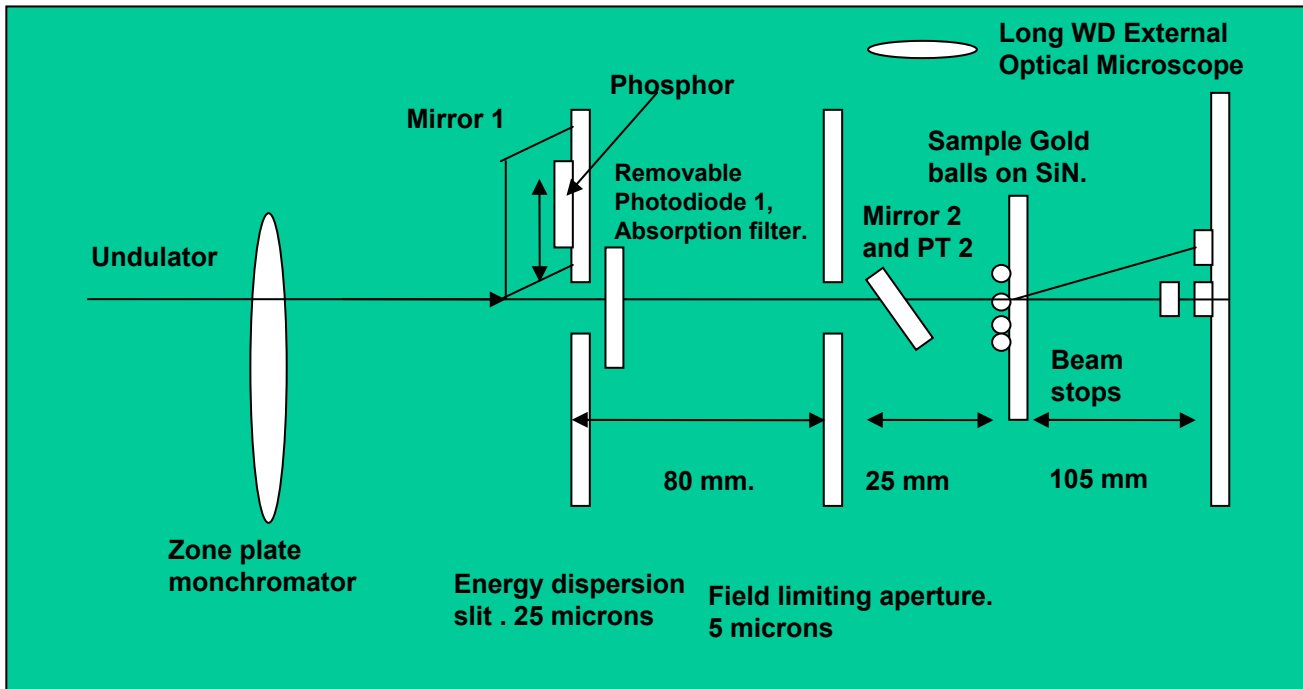


- Undulator period: 10 cm
- provides near-UV photon energies in the 1st harmonic.
- We work off the third undulator harmonic, (500 eV to 800 eV).
- An off-axis zone plate monochromator provides the necessary spectral resolving power needed. ($\lambda/\Delta\lambda = 800$) (design: M. Howells).
- Beryllium window gets rid of the unwanted 1st harmonic and separates ultra-high vacuum section of storage ring from the high-vacuum section of the endstation.
- 5 micron pinhole in the experimental chamber is placed at the positive 1st-order focus of the zone plate monochromator.

FIRST EXPERIMENTS

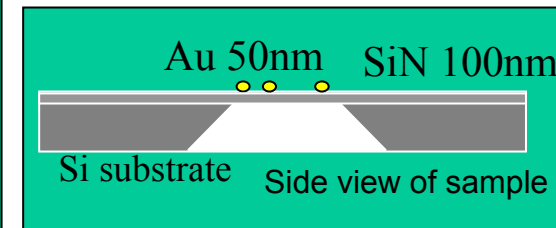


Layout of the diffraction chamber used for this experiment at BL 9.0.1 at
Advanced Light Source, LBL



Sample

Sample: 50 nm gold balls randomly distributed on SiN window (~100nm thickness and $2 \times 2 \mu\text{m}^2$)



$\lambda = 2.1 \text{ nm}$ (588 eV)

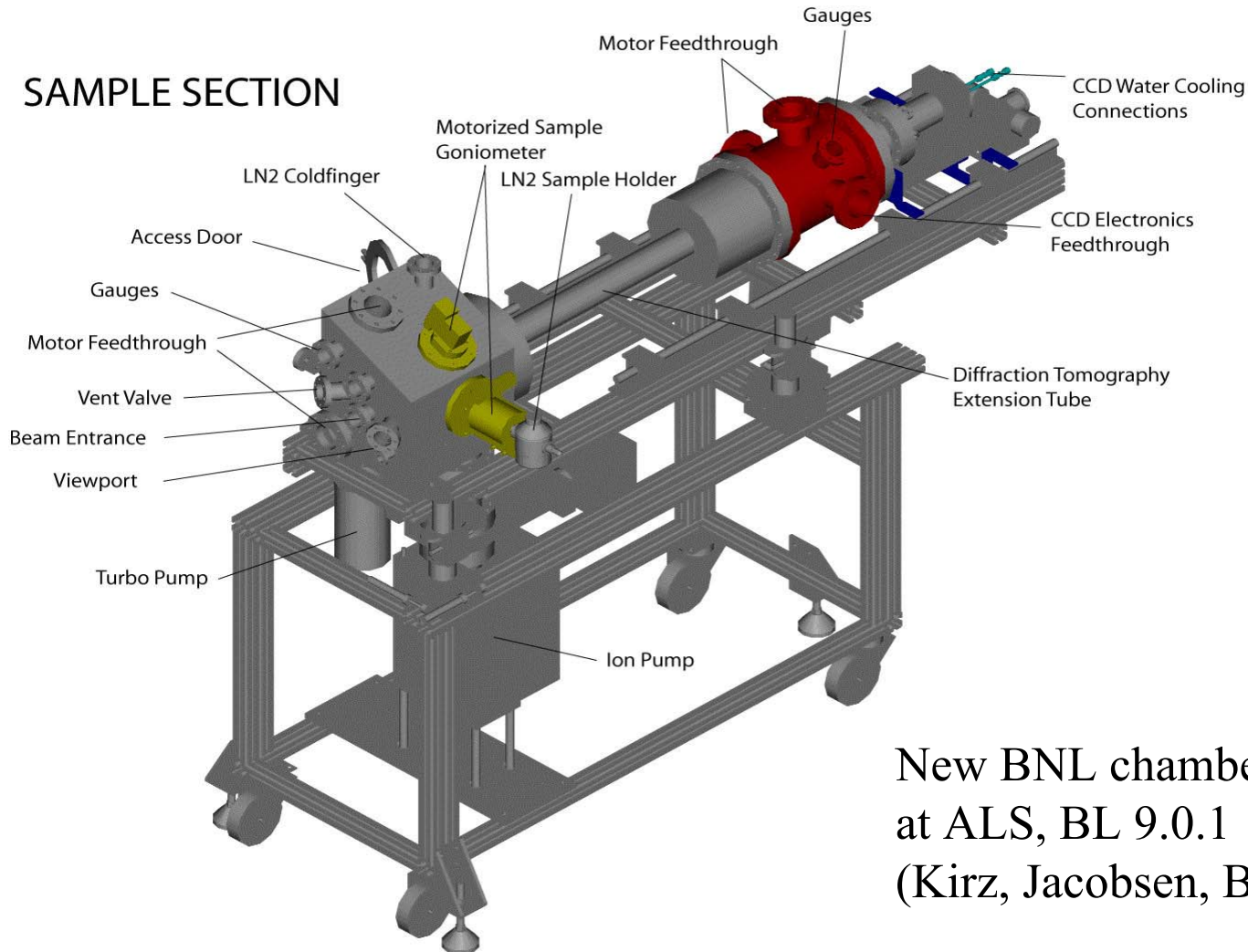
Detector: 1024×1024 Princeton back-illuminated CCD

NEW CHAMBER FROM BNL



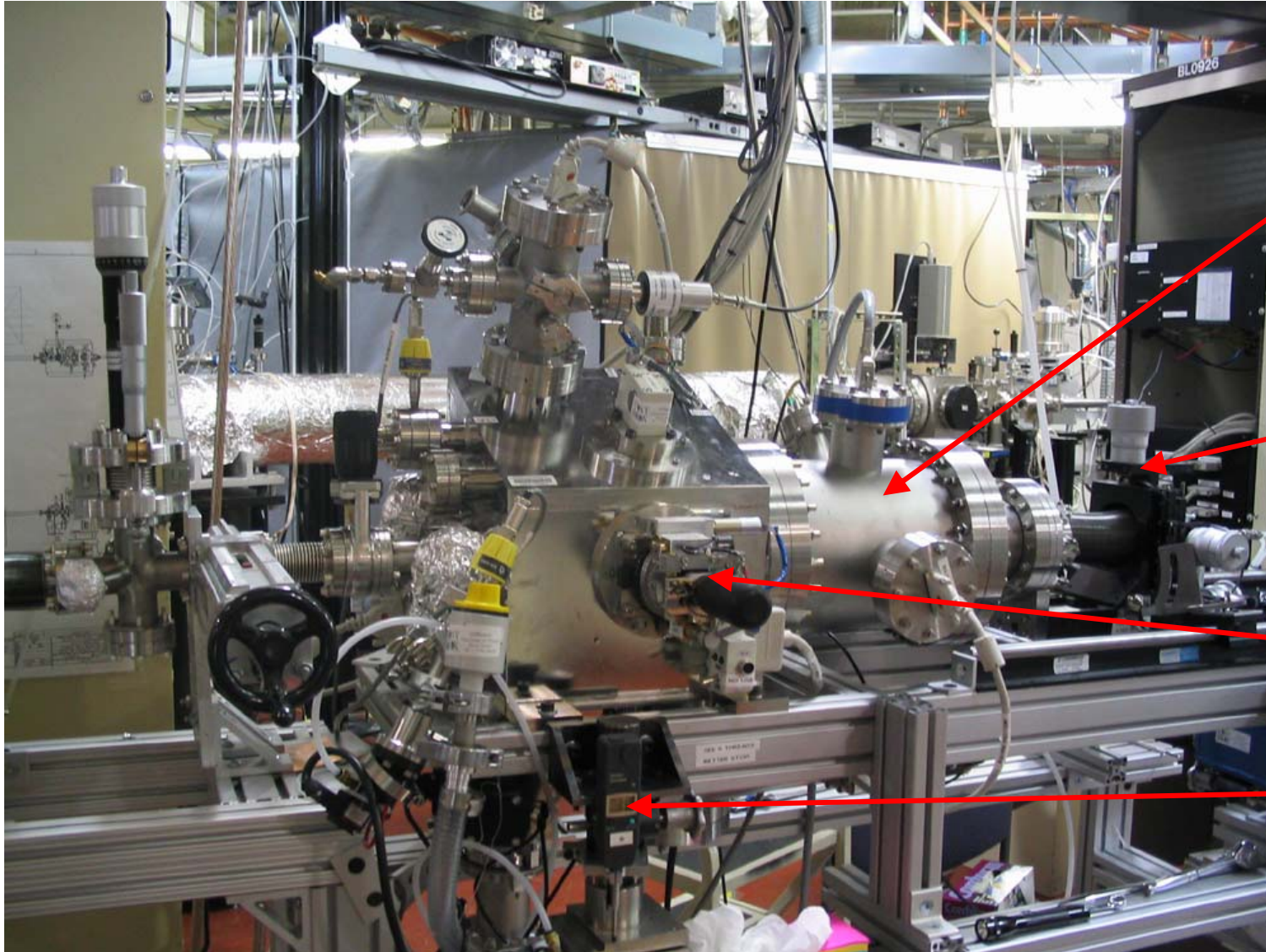
DETECTOR SECTION

SAMPLE SECTION



New BNL chamber now
at ALS, BL 9.0.1
(Kirz, Jacobsen, Beetz, Shapiro)

THE CHAMBER



CCD section

CCD
translator

Goniometer

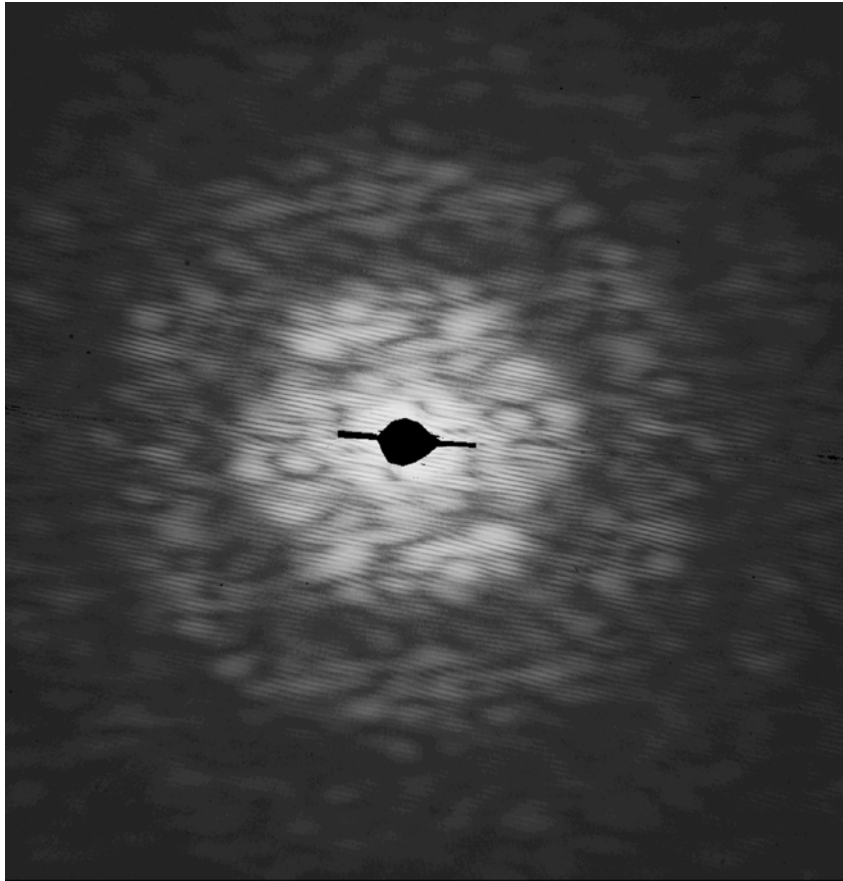
xyz-
manipulators

THE SAMPLE HOLDER



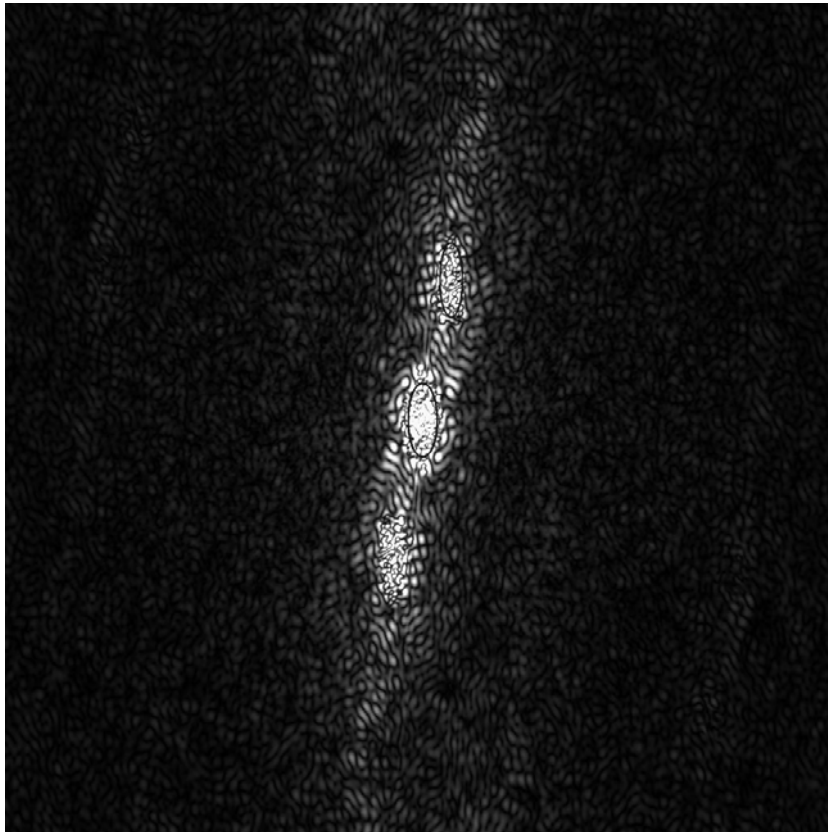
RT Tomographic sample holder built at ASU for materials applications.

DIFFRACTION PATTERN OF 50-NM GOLD BALLS RECORDED AT ALS BL 9.0.1



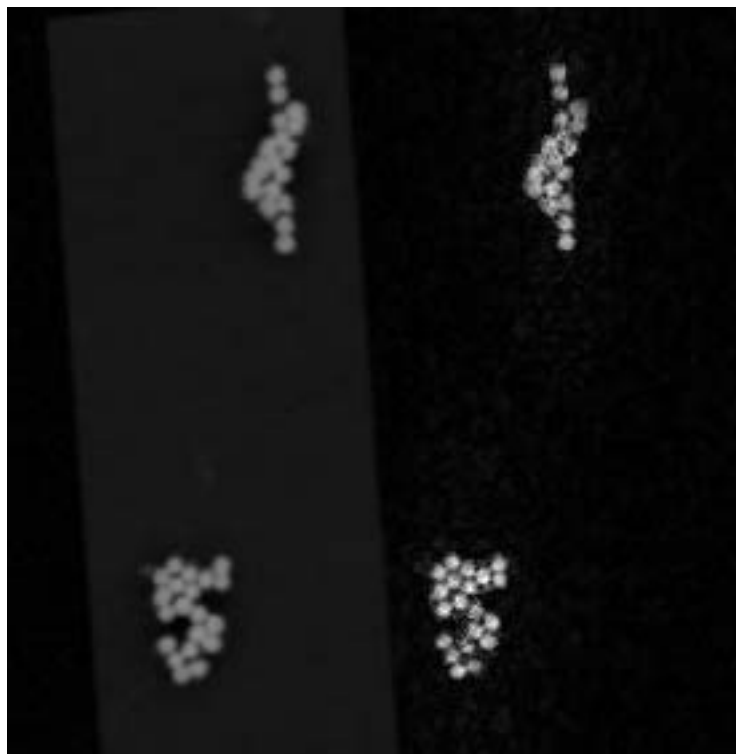
- Pattern recorded on a nude 1024×1024 by 16 bit nude CCD camera (pixel size 24 μm)
- Composite diffraction pattern obtained from six different exposure times to increase the dynamic range
- Note missing data due to beam stop in the center
- Note the fine fringes due to the fact that the object is in two separated parts implying that this recording is essentially a Fourier transform hologram and the fringes will carry the phase information

AUTOCORRELATION FUNCTION OF THE SAMPLE



- Autocorrelation of the sample obtained by taking the Fourier transform of the measured data
- Note the three concentrations of density resulting from the fact that the object is in two separated parts
- Note the autocorrelation is centrosymmetric
- The initial support derived (guessed) from this diagram is the pair of ellipses marked

RECONSTRUCTED X-RAY IMAGE AND SEM PICTURE OF THE SAMPLE FOR COMPARISON



↑
SEM

↑
X-ray
reconstruction



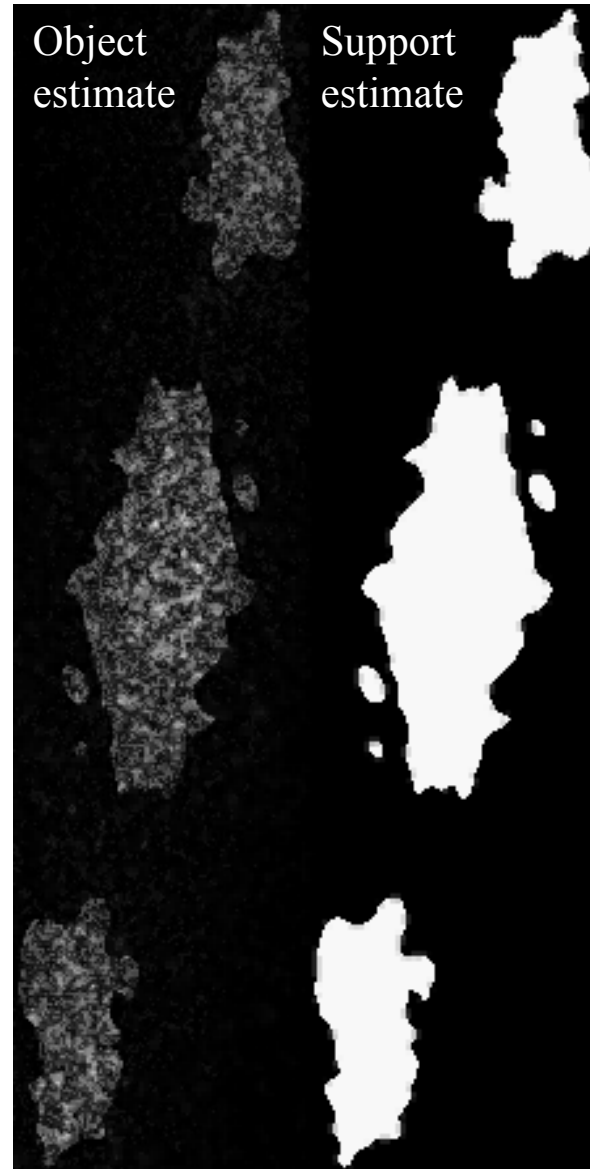
↑
Tight
support

- Sample consisting of 50 nm gold balls mounted on a 75 μm square Si_3N_4 window
- An isolated object was arranged in this form by means of sweeping away unwanted balls with an AFM. (No density outside the reconstructed area must contribute to the diffraction pattern)
- Stage 1 reconstruction using the two-ellipse support derived from the autocorrelation (100 iterations)
- Stage 2 final reconstruction using the tight support (left) derived from the preliminary form of the reconstruction (53 iterations)
- No positivity constraint was used on either real or imaginary part
- The data points blocked by beam stop were not constrained but left to float
- He et al, PRB **67**, 174114 (2003)

A NEW AND MORE POWERFUL FORM OF THE FIENUP ALGORITHM (S. Marchesini)



- Is it possible to reconstruct without any knowledge of the support?
- “SHRINKWRAP” starts by blurring and thresholding the autocorrelation function to find a support function
- Blurring is convolution with a Gaussian with $\sigma = 3$ pixels, later gradually reducing to 1.5
- Thresholding is done at 4% initially and 20% thereafter
- It then updates the support by the same means every 20 iterations
- The agreement with the previous solution and with the SEM is good
- This was real data - SHRINKWRAP also has had success with simulations of
 - grayscale objects
 - 3D objects
 - complex objects



Phase retrieval with blind support



$$|F(\mathbf{k})| = \sqrt{I(\mathbf{k})} \quad \text{known, } \varphi \text{ unknown}$$

s support estimated from Patterson function

$$p(\mathbf{r}) = \text{FFT}(I(\mathbf{k}))$$

$\beta=0.9$ feedback

$\sigma=2$ gaussian width (pixels)

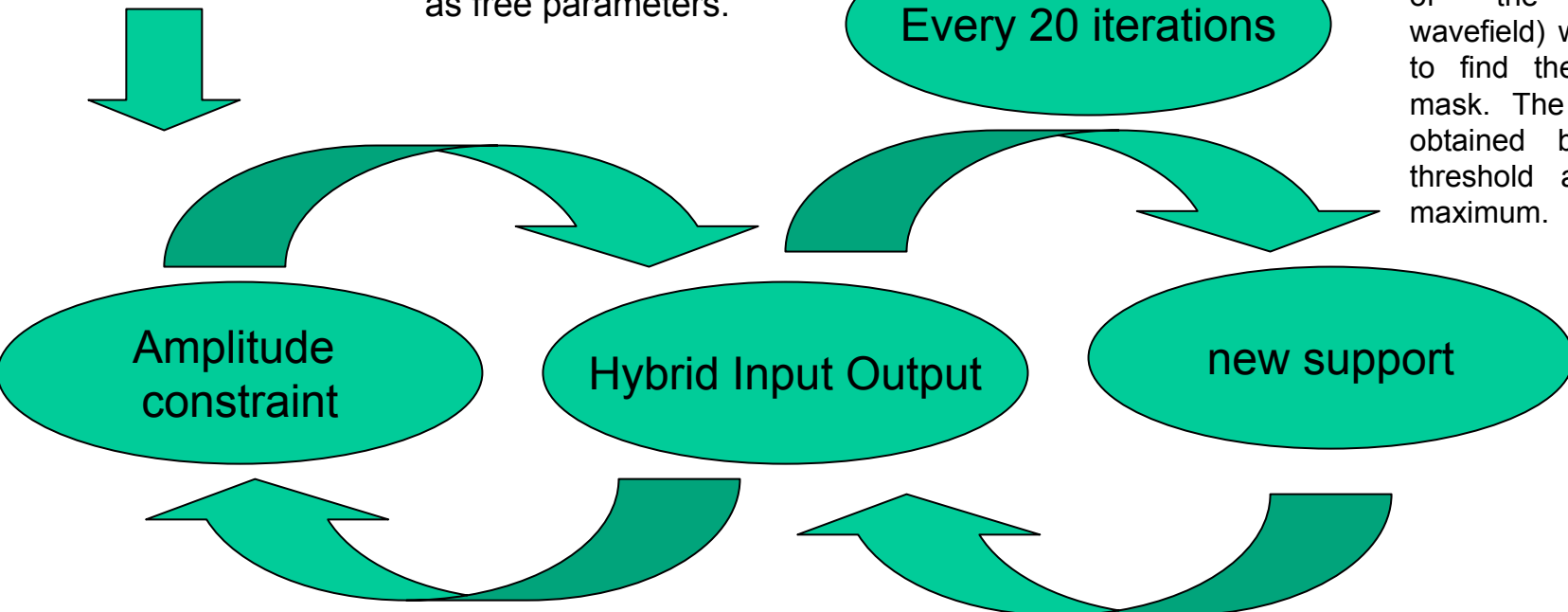
$t=0.2$ threshold

$\varphi = \text{random}$
support

Missing low frequency components are treated as free parameters.

Every 20 iterations

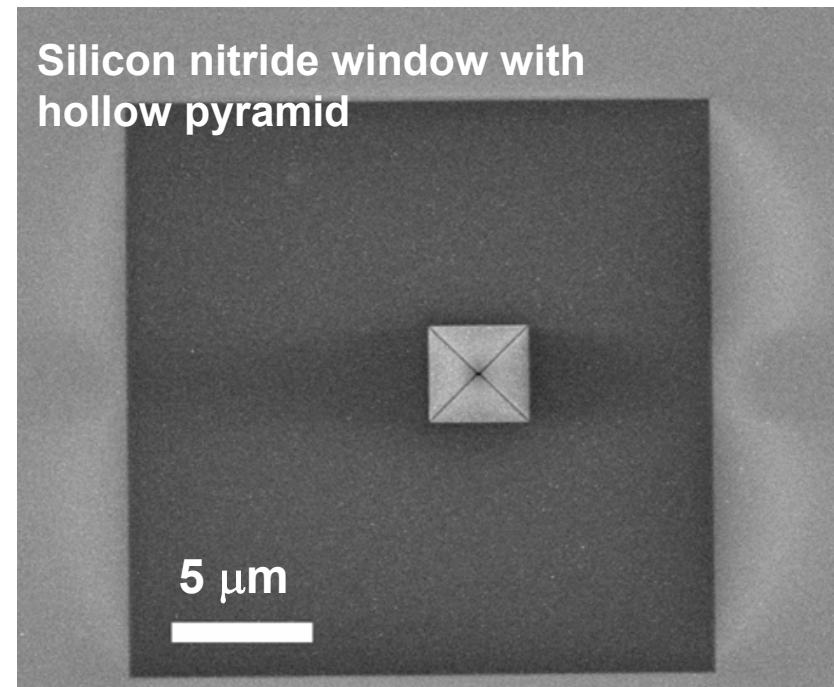
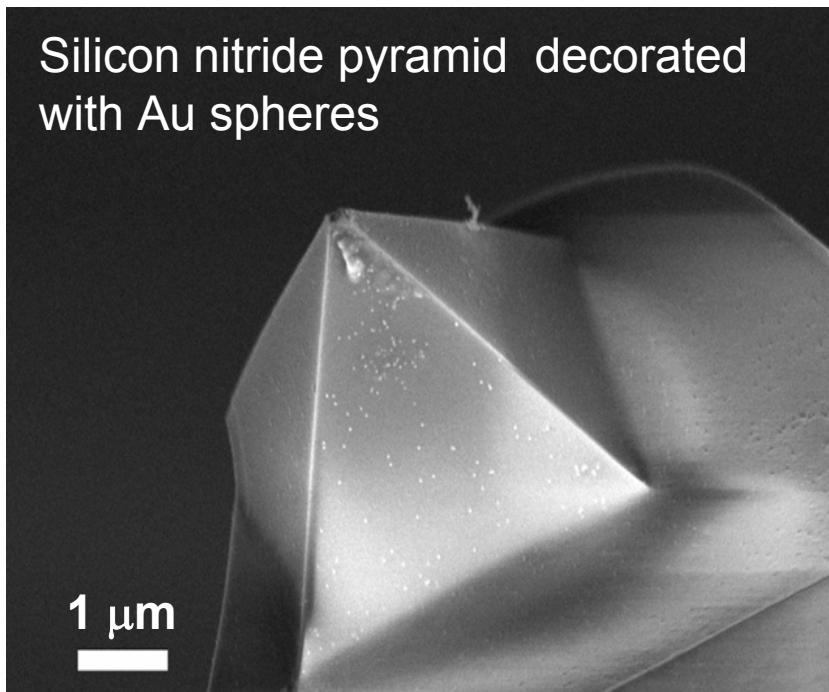
Every 20 iterations we convolve the reconstructed image (the absolute value of the reconstructed wavefield) with a Gaussian to find the new support mask. The mask is then obtained by applying a threshold at 20% of its maximum.



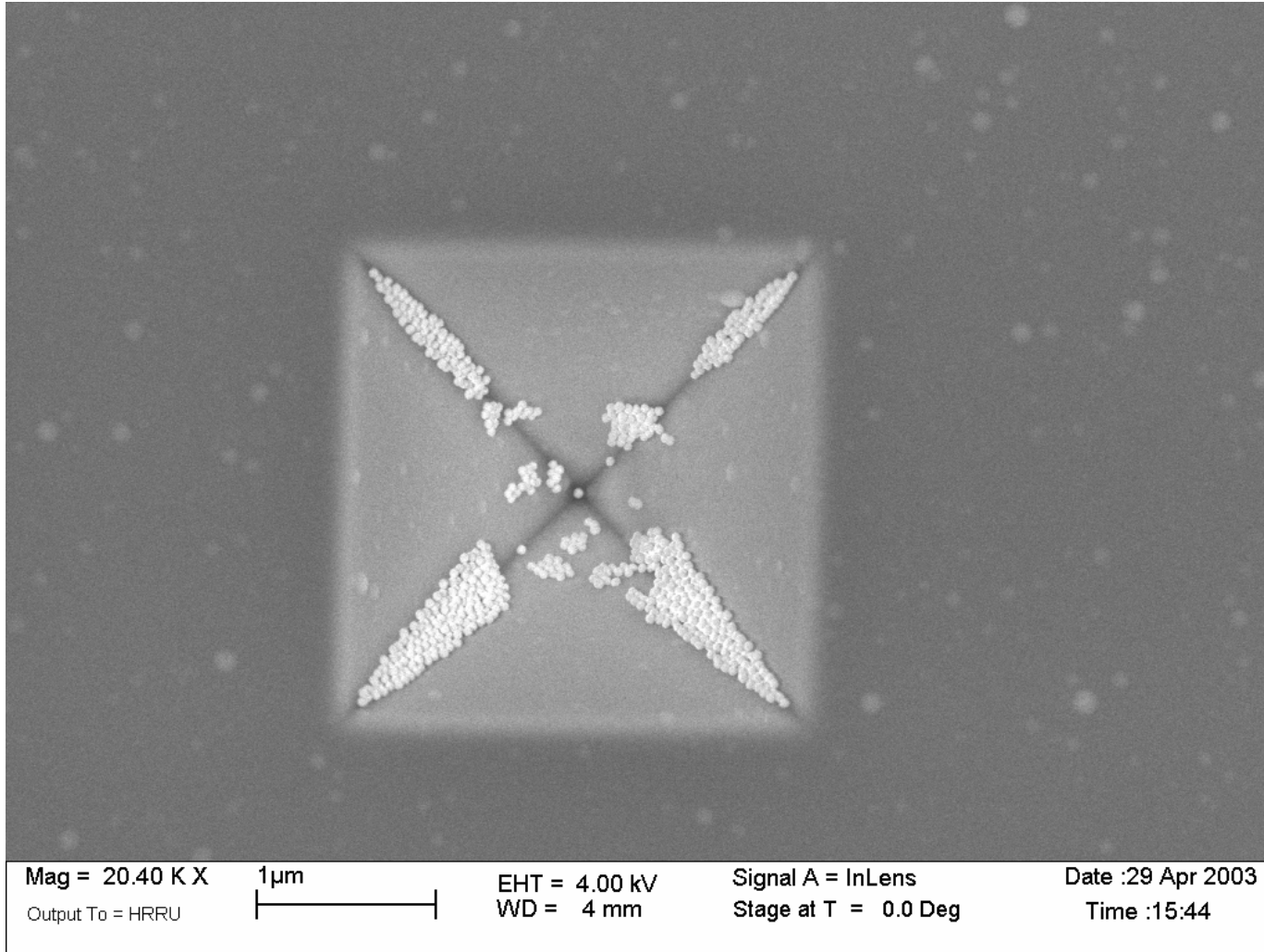
3D DIFFRACTIVE IMAGING



- Complete coverage of reciprocal space by sample rotation
- Use a true 3D object that can be well-characterized by independent means
- Will use diffraction data to test classification and alignment algorithms

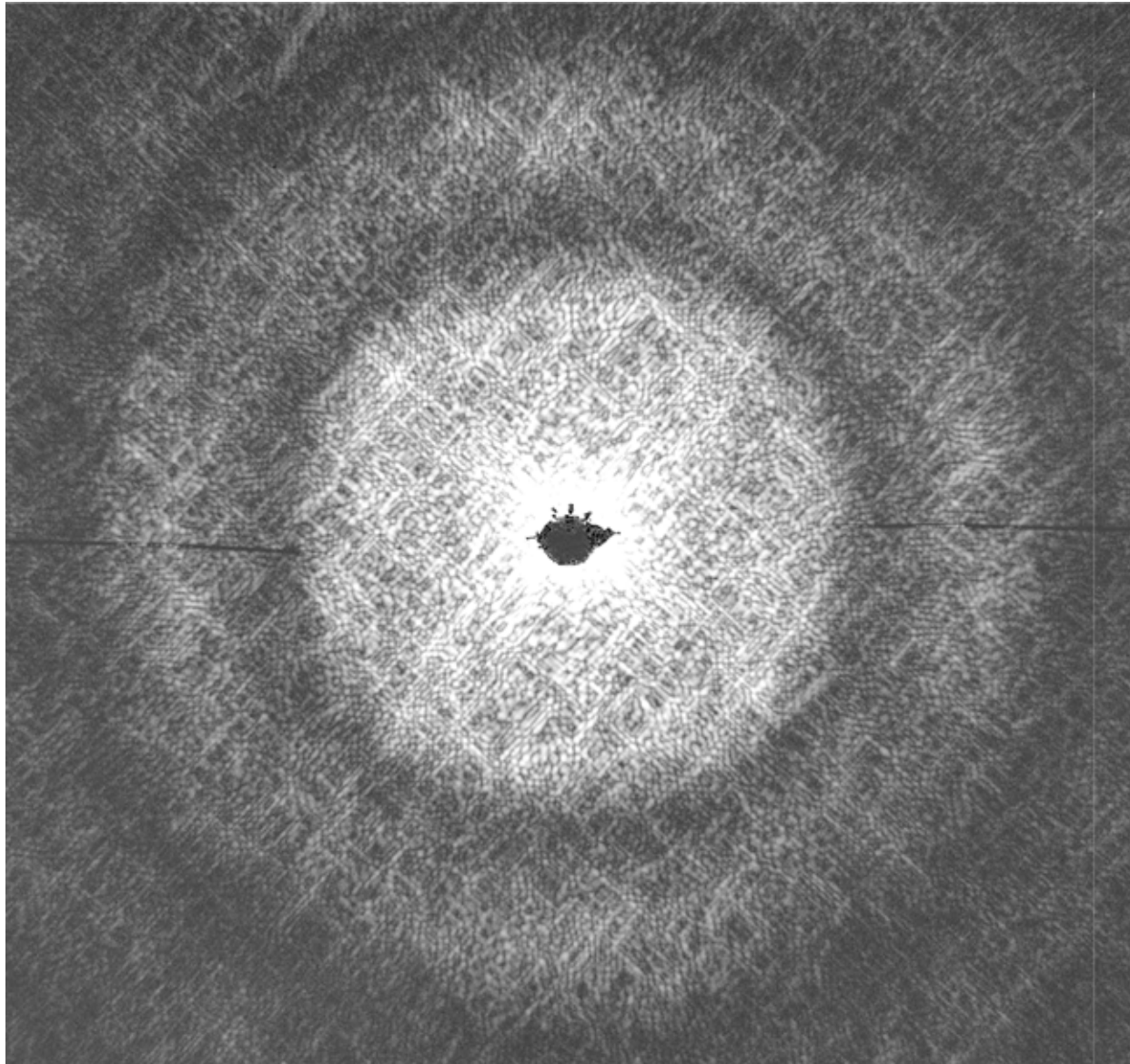


3D DIFFRACTIVE IMAGING



- SEM image of the pyramid object
- Pyramid is microfabricated in a 100 nm thick silicon nitride window and the 50 nm gold balls were dropped into the pyramid in a liquid suspension (LLNL group)

3D DIFFRACTIVE IMAGING



- 130 views: $\pm 65^\circ$ in 1° steps
- Exposures of 3, 20, and 200 seconds at each angle
- Automation is now developed to where we can take this largely unattended
- Total data collection time about 10 hours
- First 3D data set taken with the Stony-Brook-Brookhaven chamber
- Speckles are well developed and often round i. e. not radially streaked which shows that the system bandwidth is now good
- Note the envelope of the pattern is the Airy disk of one ball
- Midpoints of the sides correspond to a spatial period of 17.4 nm or a Rayleigh resolution of 8.7 nm

FOURIER TRANSFORM HOLOGRAPHY



Let \Leftrightarrow represent a Fourier transform and \otimes an autocorrelation, $*$ a convolution, then

$$\text{If } f(x) \Leftrightarrow F(k)$$

$$\text{Then } f(x) \otimes f(x) = f(x) * f^*(-x) \Leftrightarrow |F(k)|^2$$

- Now $f(x) \otimes f(x)$ is twice as wide as $f(x)$
- Therefore the Shannon sampling interval of its transform will be half as great
- Suppose now that we have a double object: $f(x) = g(x) + \delta(x - b)$
- The last equation can then be written

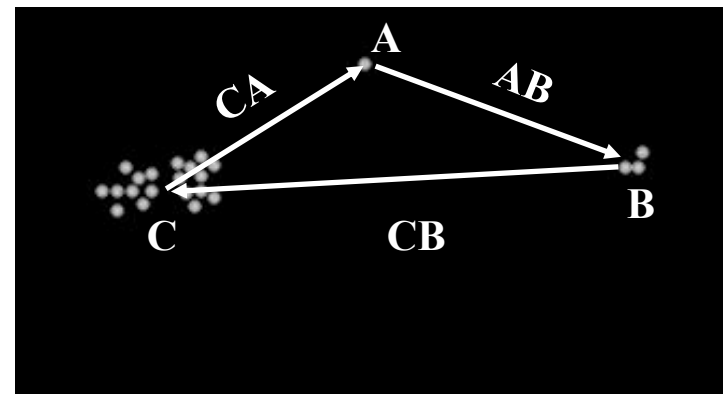
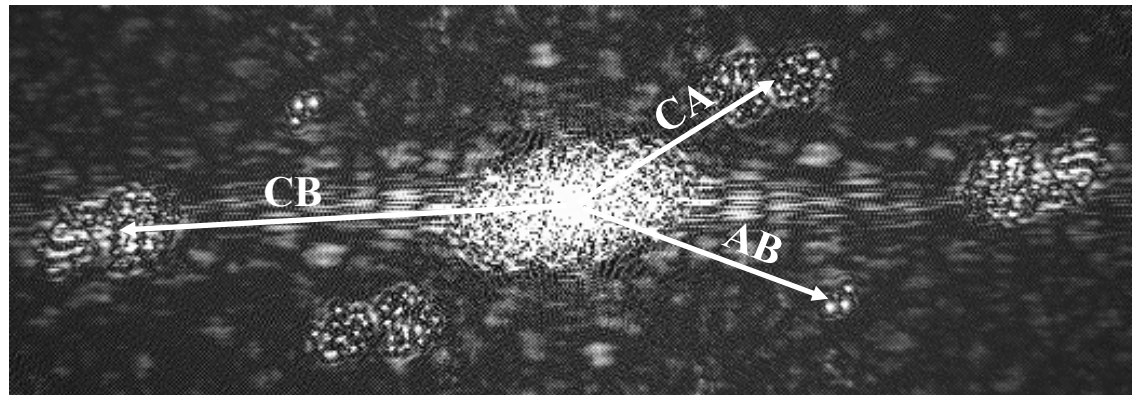
$$\begin{aligned} |F(k)|^2 \Leftrightarrow f(x) * f^*(-x) &= [g(x) + \delta(x - b)] * [g(-x) + \delta(x + b)]^* \\ &\Leftrightarrow g(x) \otimes g(x) + g(x + b) + g^*(-x - b) + \delta(x) \end{aligned}$$

- A simple Fourier transform of the diffraction pattern returns the autocorrelation of the object plus the two (complex) twin images and all three are separated if b is large enough - Fourier-transform holography - see later
- Normally you cannot recover a function from its autocorrelation but here you can
- If the delta function is replaced by a spike of finite width then the images will be convolved with the spike

FOURIER TRANSFORM HOLOGRAPHY



- Example from our earliest experiments
- Autocorrelation of the object found by taking the Fourier transform of the measured diffraction pattern
- Shows the role of separation of parts in determining the support from the autocorrelation
- Since element A is a single ball we see images and twin images of the other two elements formed by Fourier transform holography with a resolution of one ball size (50 nm in this case)



Sketch of the object to explain the features of the autocorrelation

DOSE AND FLUX SCALING WITH RESOLUTION



M. Howells et al. calculated the coherent scattering cross section of a cubic voxel and thence the dose D required to produce P scattered x-rays into a detector with collection angle chosen for resolution d with the following result

$$D = \frac{\mu P h \nu}{\varepsilon} \frac{1}{r_e^2 \lambda^2 |\rho|^2 d^4} \quad \text{Fluence} = \frac{P}{r_e^2 \lambda^2 |\rho|^2 d^4}$$

Fluence: total photons per unit area

Dose: absorbed energy per unit mass)

μ = the voxel intensity absorption coefficient

$h\nu$ = the photon energy

r_e = the classical electron radius

λ = the photon wave length

ρ = the scattering strength of the voxel material in electrons per unit volume

ε = the density, P = # of quanta into detector from voxel ($P = N\sigma$ for flux N incident quanta/area)

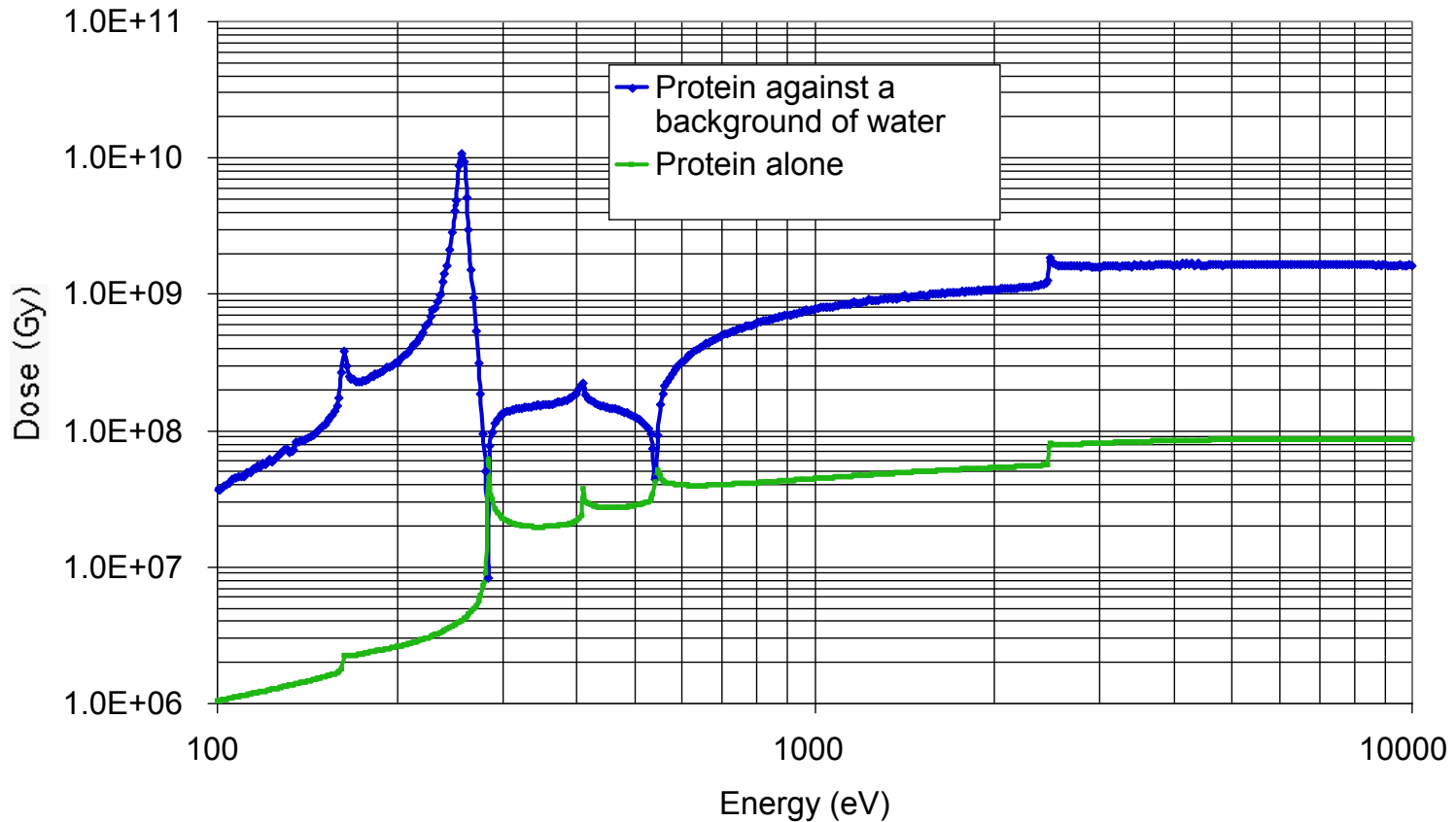
The dose and fluence scales as the inverse fourth power of the resolution

$$D = \mu P h \nu / \varepsilon \sigma \quad \text{Joule/kgm}, \quad T \sim \text{Fluence} / \text{Incident flux} \quad \sigma_s = \pi r_e^2 \theta^2 \left| \sum_m \tilde{f}_m \right|^2 = \pi r_e^2 \lambda^2 |\rho|^2 d^4 \quad || = (\rho d^3)^2$$

DOSE REQUIREMENTS (M. Howells)



Below is the dose to detect a 10 nm voxel made of protein according to the Rose criterion plotted against x-ray energy. A detector collecting an angle chosen for 10 nm resolution is assumed

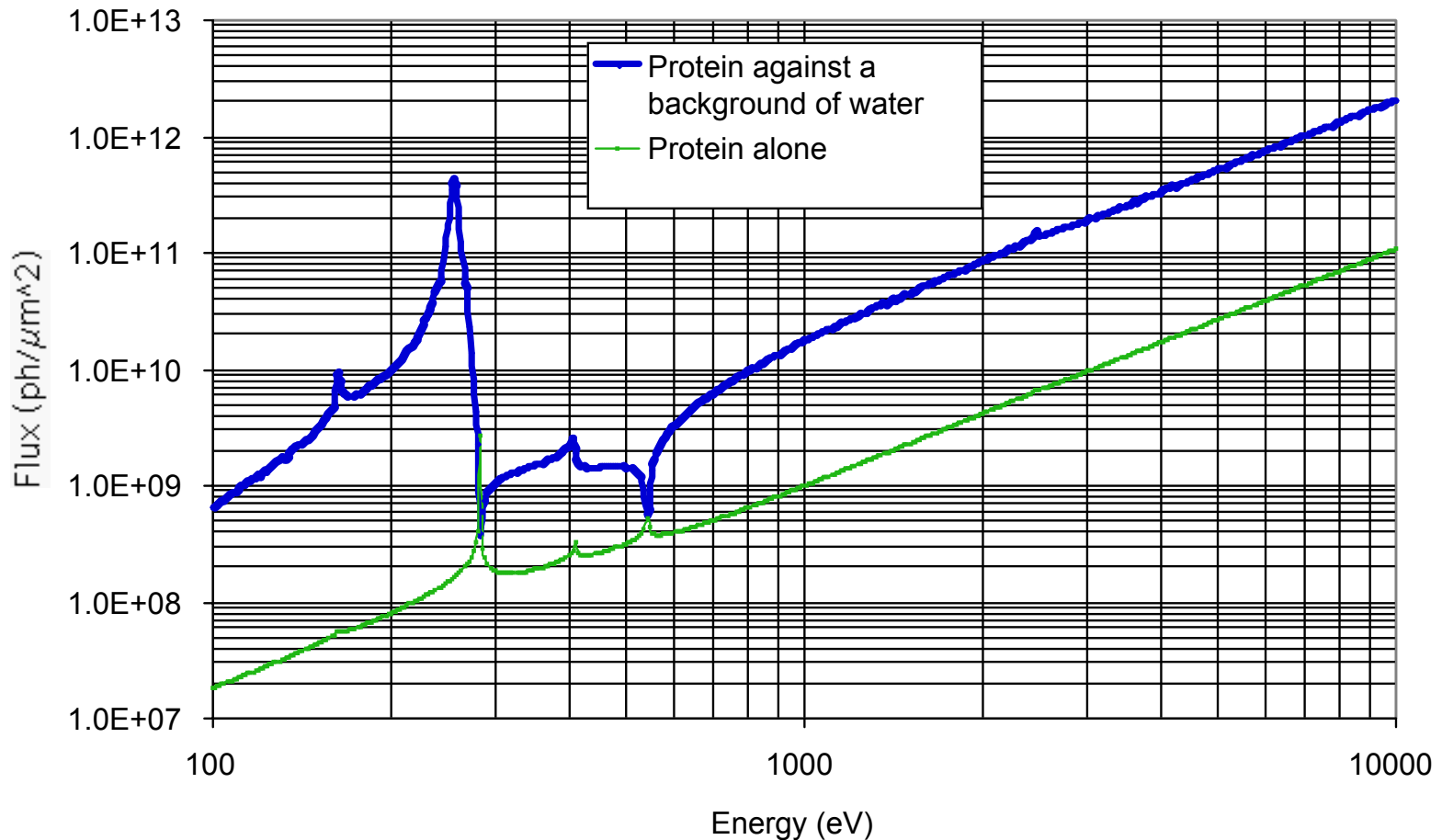


Conclude: energy doesn't matter much

FLUX REQUIREMENTS (M. Howells)



Flux to detect a 10 nm voxel made of protein according to the Rose criterion plotted against x-ray energy. A detector collecting an angle chosen for 10 nm resolution is assumed



Conclude: Energy does matter.

WHAT IS THE BEST WAVELENGTH?



FLUX CONSIDERATIONS:

- A. The required fluence is $P/[r_e^2 \lambda^2 |\rho|^2 d^4]$ which scales like λ^{-2} (coming from the voxel cross section so this is neglecting $|\rho|^2$ dependence) (unfavorable to HXR)
- B. For a given source brightness B the coherent flux available is $B (\lambda/2)^2$ (unfavorable to HXR)
- This implies a fourth-power fluence penalty for increasing the x-ray energy

DOSE CONSIDERATIONS:

- The dose for light elements is roughly flat with wavelength

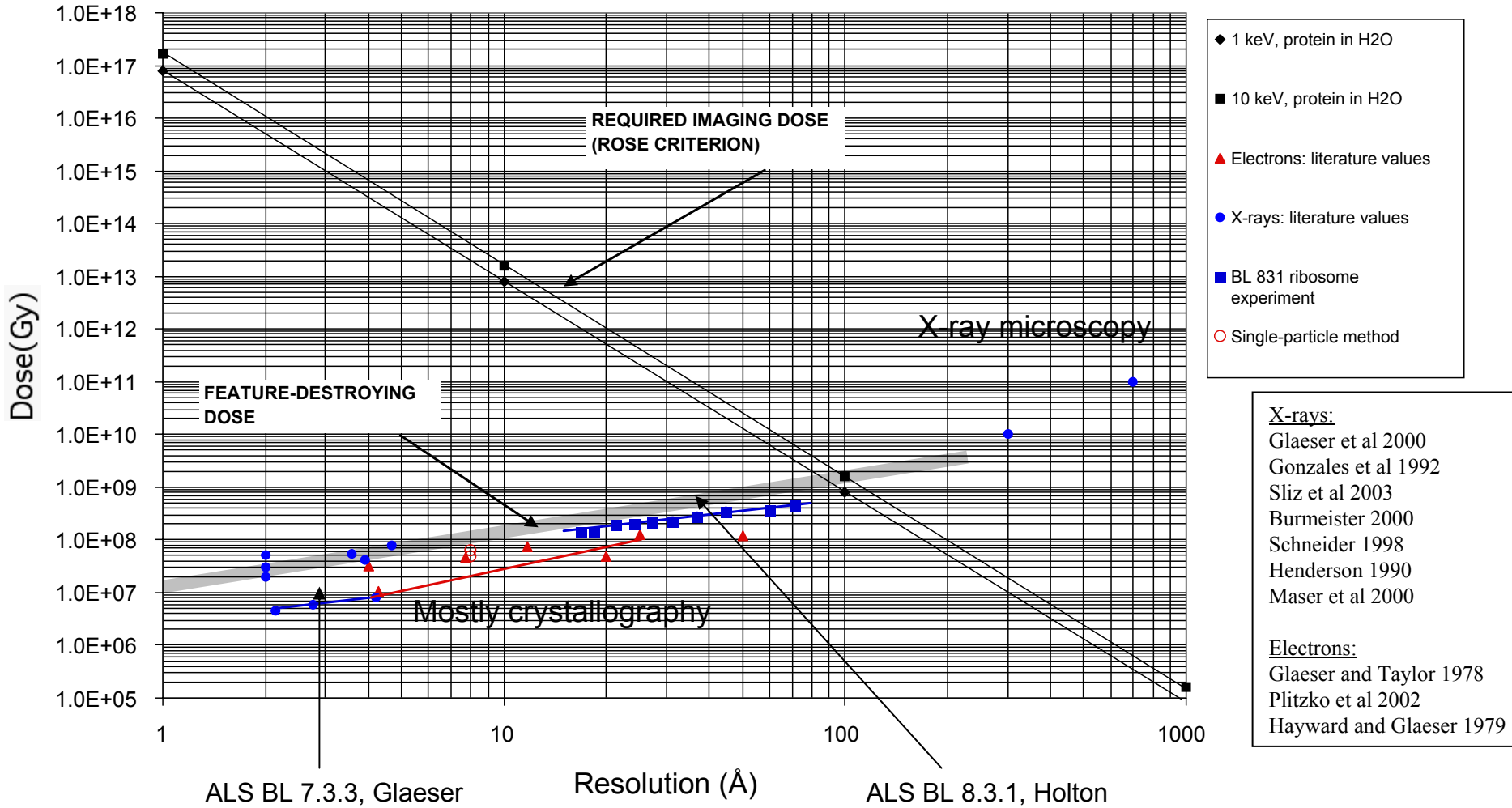
DIFFRACTION CONSIDERATIONS:

- Therefore one should use the lowest possible x-ray energy consistent with (roughly) $\lambda < d/2$

RECONSTRUCTION CONSIDERATIONS

- Harder x-rays will make the scattering density essentially real.
- These are not the only considerations (Phase contrast ? Thicker samples ?) - ongoing discussions suggest around 1 - 2 keV

DOSE-RESOLUTION RELATIONSHIP FOR 3D IMAGING OF FROZEN-HYDRATED SAMPLES



- X-rays:
 Glaeser et al 2000
 Gonzales et al 1992
 Sliz et al 2003
 Burmeister 2000
 Schneider 1998
 Henderson 1990
 Maser et al 2000
- Electrons:
 Glaeser and Taylor 1978
 Plitzko et al 2002
 Hayward and Glaeser 1979

of dose against resolution. Falling line: dose resulting from an x-ray illumination just sufficient for the voxel detectable according to the Rose criterion. Single particle experiments are only possible *above* the “required imaging dose” line and *below* the “feature-destroying dose” line

Current capability and applications



- Stony Brook/NSLS chamber @ BL 9.0.1
 - Incorporates low resolution X-ray microscope
 - Provision for frozen hydrated samples
 - Precision positioning and rotation of specimen, optics
- Stony Brook Goals:
 - Develop technique (recording and reconstruction)
 - Study dose vs resolution; damage limits
 - 3D reconstruction of frozen hydrated dwarf yeast cell
- **ASU/ALS/LLNL Goals:**

Use mainly for mat. sci. applications (mesoporous, framework and "labyrinth" structures, **stardust**, aerosols, **glassy foams** (hydrogen storage UCSB Galen **Stuckey**), cavities in steels, Line defect imaging in "thick" samples (work hardening), precipitate arrangement in "thick" alloys.
- In biology at 5nm: Multimolecular aggregates, Mitochondria, Organelle, Viruses - T4 phage

Recent developments



- Better HiO algorithms appeared at Cairns - Elsner, Luke. (Density constraint, Hilbert transforms).
- How to tell whether algorithm converged.
 - Error metrics. CC vs HiO error.
- How to optimize use of computer resources?
 - Want faster 1024^3 FFT. Network bottleneck. FFT hardware bought at ASU. (Currently 1 sec for $1K^2$ FFT. Need 100 itns).
- Zone plate imaging in new chamber gives excellent "support". Combine with "Shrinkwrap".
- "Prepared objects" and FTH are powerful - use Kleindiek manipulator to place gold ball near object, use thin SiN cantilevers as support membrane to enable higher tilts, make small (50-100nm) platinum dot for FTH.